EUMETSAT

OSI SAF

OCEAN AND SEA ICE

Algorithms Theoretical Basis Document for the Geostationary Satellite Radiative Fluxes

GOES-16	OSI-305-b	OSI-306-b
Meteosat-11	OSI-303-a	OSI-304-a
Meteosat-9	OSI-IO-DLI	OSI-IO-SSI

Version : 1.2

Date : 5/7/2022

METEO FRANCE

Document Change record

Document version	Date	Author	Change description
0.1	11/03/2019	MF/CMS	Initial submitted version This document supersedes the ATBD for the GOES-16 radiative fluxes and contains also the information relative to Meteosat radiative fluxes.
0.2	23/04/2019	CH	Some typo corrected. Precision added on "radiometer count"
1.0	06/05/2019	AM	GOES-16 calibration correction updated in 2.5.2
1.1	12/11/2019	AM	Precision added on hourly calculation time schedule in 4.2
1.2	5/7/2022	SSP	Switch to Meteosat-9 over Indian Ocean.

Contents

1. Introduction

1.1. Scope of the document

The EUMETSAT Satellite Application Facilities (SAFs) are dedicated centres of excellence for processing satellite data. They form an integral part of the distributed EUMETSAT Application Ground Segment. The Ocean and Sea Ice SAF, led by Météo-France/Centre de Météorologie Spatiale (MF/CMS), has the responsibility of developing, validating and distributing products of near real time products of Sea Surface Temperature (SST), radiative fluxes, wind and Sea Ice parameters for a variety of platforms/sensors. More information can be found at http://www.osi-saf.org.

As part of the Third Continuous Development and Operations Phase (CDOP 3) OSI SAF (more specifically MF/CMS) has committed to provide user community with operational product of Sea Surface Temperature (SST) and Radiative Fluxes from the American Geostationary Operational Environment Satellite (GOES) in East position and the Meteosat Second Generation (MSG) in position 0°. OSI SAF is also providing SST and radiative fluxes for MSG Indian Ocean on a best effort basis. Currently OSI SAF is processing data from:

- GOES-16 which was launch on the 19th of November 2017 and was declared operational in East position (75.2 ◦ W) on the 18th of December 2017.
- Metosat-11 which was launched on the 15th of July 2015 and operationally replaced Meteosat-10 on the 20th of February 2018.
- Meteosat-9 which has operationally replaced Meteosat-8 over Indian Ocean in 45.5 E on the 23rd of June 2022.

This document describes the algorithms and the main features of the processing of the radiative fluxes derived from geostationary satellite data.

1.2. Definitions and acronyms

The Surface Solar Irradiance (SSI) is the solar irradiance reaching the Earth surface in the 0.3-4 μm band, the irradiance being the radiant flux received per unit area.

The Downward Longwave Irradiance (DLI) is the irradiance reaching the Earth surface in the 4-100 μm band.

ABI	Advanced Baseline Imager
BDRF	bi-directional reflectance function
CERES	Clouds and Earth's Radiant Energy System
CMS	Centre de Météorologie Spatiale
CM SAF	Climate SAF
DLI	Downward Longwave Irradiance
ECMWF	European Center for Medium range Weather Forecast
GOES	Geostationary Operational Environmental Satellite
GOES-E	GOES East
FDC	Full Disk Coverage
LML	Low and Mid Latitudes

LSA SAF	Land Surface Analysis SAF
MDS	Match up Data Set
MSG	Meteosat Second Generation
NWC SAF	Nowcasting and very short range forecasting SAF
OSI SAF	Ocean and Sea Ice SAF
RTM	Radiative Transfer Model
SAF	Satellite Application Facility
SEVIRI	Spinning Enhanced Visible and Infrared Imager
SSI	Surface Solar Irradiance
SST	Sea Surface Temperature
TOA	Top of atmosphere
UT	Universal Time

1.3. Reference documents

[RD.1] Algorithm Theoretical Basis Document for the Cloud Product Processors of the NWC/GEO, version 10d
NWC/CDOP2/GEO/MFL/SCI/ATBD/Cloud

[RD.2] Radiative Fluxes Validation Report – OSI-305a / OSI-306a / OSI-303 / OSI-304 / OSI-IO-DL I/ OSI-IO-SSI
SAF/OSI/CDOP3/MF/SCI/RP/328

[RD.3] OSI SAF HALF-YEARLY OPERATIONS REPORT, 2st half 2018.
SAF/OSI/CDOP3/MF/TEC/RP/29

1.4. Applicable documents

[AD.1] OSI SAF, Product Requirements Document, version 1.4, 20/12/2018
SAF/OSI/CDOP3/MF/MGT/PL/2-001

1.5. Scientific background

The radiative fluxes over ocean are mainly used as input to numerical ocean models or to biological studies (chlorophyll blooms, aquaculture). The accuracy requirements on the hourly GOES-East radiative fluxes [AD.1] are: a 10 % bias and 30 % standard-deviation for the solar flux and a 5 % bias and 10 % standard-deviation for the longwave flux, the percentages being relative to the mean value and the statistics being on a monthly period.

Radiative flux retrievals from satellite data has begun in the 1980s, processing various satellites and instruments. The retrieval methods can be separated into two types: parameterizations (Tarpley, 1979, Gautier et al., 1980, Darnell et al., 1992) and Radiative Transfer Model (RTM) calculations (Schmetz, 1989; Pinker and Laszlo, 1992; Hollman et al.,2006).

The OSI SAF SSI algorithm is a physical parameterization applied to a visible channel (Meteosat or GOES-East radiometer), after Gautier et al. 1980 and Frouin and Chertock, 1992. The LSA SAF follows the same method as OSI SAF, but using three SEVIRI channels instead of one and an actual surface albedo (Geiger et al. 2008) and the CM SAF follows a RTM approach (Hollman et al.,2006).

The OSI SAF DLI algorithm is a bulk parameterization using air temperature and humidity predicted by a NWP model and cloud information derived from satellite data. Bulk parameterizations are commonly used for air-sea interface studies based on meteorological observations, while satellite methods are often based on RTM calculations. The LSA SAF follows a bulk parameterization and the CM SAF a RTM approach.

The OSI, CM and LSA SAF radiative fluxes have been compared and validated against in situ measurements, over Europe (Ineichen et al., 2009) and over Africa (Ineichen, 2010), with a focus on SSI as the pyrgeometer measurements were too few. The two studies conclude that the products from the different SAFs have comparable biases and precisions, showing that the OSI SAF parameterizations compare favourably with the more complex RTM methods.

1.6. Radiometer characteristics

MSG payload include the SEVIRI instrument. The SEVIRI radiometer is a multi-channel passive imaging radiometer operating in twelve channels (table 1). The full disk is scanned with a repeat cycle of 15 minutes.

GOES-16/ABI is a multi-channel passive imaging radiometer operating in sixteen channels (table 2). The full disk is scanned with a basic repeat cycle of 15 minutes, but a cycle at 10 minutes has been used occasionally.

Channel No.	Spectral Band (μm)	Characteristics of Spectral Band (μm)			Main observational application
		λ_{cen}	λ_{min}	λ_{max}	
1	VIS0.6	0.635	0.56	0.71	Surface, clouds, wind fields
2	VIS0.8	0.81	0.74	0.88	Surface, clouds, wind fields
3	NIR1.6	1.64	1.50	1.78	Surface, cloud phase
4	IR3.9	3.90	3.48	4.36	Surface, clouds, wind fields
5	WV6.2	6.25	5.35	7.15	Water vapor, high level clouds, atmospheric instability
6	WV7.3	7.35	6.85	7.85	Water vapor, atmospheric instability
7	IR8.7	8.70	8.30	9.1	Surface, clouds, atmospheric instability
8	IR9.7	9.66	9.38	9.94	Ozone
9	IR10.8	10.80	9.80	11.80	Surface, clouds, wind fields, atmospheric instability
10	IR12.0	12.00	11.00	13.00	Surface, clouds, atmospheric instability
11	IR13.4	13.40	12.40	14.40	Cirrus cloud height, atmospheric instability
12	HRV	Broadband (about 0.4 – 1.1 μm)			Surface, clouds

Table 1: Spectral channel characteristics of SEVIRI in terms of central, minimum and maximum wavelength of the channels and the main application areas of each channel http://oiswww.eumetsat.org/WEBOPS/msg_interpretation/msg_channels.php

TABLE 1. Summary of the wavelengths, resolution, and sample use and heritage instrument(s) of the ABI bands. The minimum and maximum wavelength range represent the full width at half maximum (FWHM or 50%) points. [The Instantaneous Geometric Field Of View (IGFOV).]

Future GOES imager (ABI) band	Wavelength range (μm)	Central wavelength (μm)	Nominal subsatellite IGFOV (km)	Sample use	Heritage instrument(s)
1	0.45–0.49	0.47	1	Daytime aerosol over land, coastal water mapping	MODIS
2	0.59–0.69	0.64	0.5	Daytime clouds fog, insolation, winds	Current GOES imager/ sounder
3	0.846–0.885	0.865	1	Daytime vegetation/burn scar and aerosol over water, winds	VIIRS, spectrally modified AVHRR
4	1.371–1.386	1.378	2	Daytime cirrus cloud	VIIRS, MODIS
5	1.58–1.64	1.61	1	Daytime cloud-top phase and particle size, snow	VIIRS, spectrally modified AVHRR
6	2.225–2.275	2.25	2	Daytime land/cloud properties, particle size, vegetation, snow	VIIRS, similar to MODIS
7	3.80–4.00	3.90	2	Surface and cloud, fog at night, fire, winds	Current GOES imager
8	5.77–6.6	6.19	2	High-level atmospheric water vapor, winds, rainfall	Current GOES imager
9	6.75–7.15	6.95	2	Midlevel atmospheric water vapor, winds, rainfall	Current GOES sounder
10	7.24–7.44	7.34	2	Lower-level water vapor, winds, and SO_2	Spectrally modified current GOES sounder
11	8.3–8.7	8.5	2	Total water for stability, cloud phase, dust, SO_2 rainfall	MAS
12	9.42–9.8	9.61	2	Total ozone, turbulence, and winds	Spectrally modified current sounder
13	10.1–10.6	10.35	2	Surface and cloud	MAS
14	10.8–11.6	11.2	2	Imagery, SST, clouds, rainfall	Current GOES sounder
15	11.8–12.8	12.3	2	Total water, ash, and SST	Current GOES sounder
16	13.0–13.6	13.3	2	Air temperature, cloud heights and amounts	Current GOES sounder/ *GOES-12+* imager

Source: Schmit, T.J., Gunshor, M.M., Menzel, W.P., Gurka, J.J., Li, J., Bachmeier, A.S., 2005, Introducing the Next-Generation Advanced Baseline Imager on GOES-R, Bulletin of the American Meteorological Society, v. 86, p. 1079-1096.

Table 2 : channels of ABI instrument https://www.goes-r.gov/spacesegment/ABI-tech-summary.html

2. SSI algorithm

The OSI SAF physical parameterization is applied separately to every pixel of a satellite image. The various steps of the method are presented below.

2.1. Calibration

The signal measured by each detector of a radiometer is digitized into a number called "count". The radiometer 0.6 μm visible count is converted into a bi-directional reflectance. The formulation of equation (1) depends on the instrument (see 2.5).

$$L_{sc} = L_{sc}(t, C) \quad (1)$$

$$R_{nb} = L_{sc} / (\nu(j) \mu_0) \quad (2)$$

$$\nu(j) = 1 + 0.0334 \cos[2\pi (j-2) / 365.25] \quad (3)$$

with

L_{sc} : scaled radiance i.e. radiance divided by the solar spectral irradiance convoluted with the radiometer filter

R_{nb} : narrowband reflectance (relative to the band of the radiometer spectral filter)

C : radiometer count

t : current time (julian day)

$\mu_0 = \cos(\theta_0)$ θ_0 being the sun zenith angle

$\nu(j)$: corrective term accounting for the Earth-sun distance seasonal variation, j is the day of year

2.2. Narrow to broadband conversion

The reflectance relative to the narrow band of the radiometer spectral filter is converted into the reflectance relative to the broadband of the solar spectrum. As proposed in Pinker and Lazlo, 1992, this conversion is made with a linear formula :

$$R = M R_{nb} + B \quad (4)$$

where the M and B coefficients depend on the scene type. Instead of one type “cloud” as in Pinker and Lazlo, 1992, several types of clouds have been introduced, since the reflectances of fractional and semi-transparent clouds vary with the underlying surface.

2.3. Anisotropy correction

The broadband bi-directional reflectance is converted into the Top Of Atmosphere (TOA) albedo, which is independent of satellite viewing angle. This step is based on the Manalo-Smith et al. 1998 formulas (derived from Earth Radiation Budget Instrument data), where the anisotropic factor is an analytical function of the viewing angles depending on the scene type.

$$A(\theta_0) = R / f_{aniso} \quad (5)$$

with

A : TOA albedo

R : broadband reflectance

f_{aniso} : anisotropic factor or bi-directional reflectance function (BDRF)

2.4. SSI parameterization

2.4.1. TOA albedo to SSI

The SSI parameterization separates clear sky and cloudy sky cases, which are identified by the cloud classification of the Nowcasting (NWC) SAF [RD.1]. The equations, after Gautier et al, 1980, are the following:

if clear $E = E_0 \, \nu(j) \, \mu_0 \, T_a$ (6)

if cloudy $E = E_0 \, \nu(j) \, \mu_0 \, T_1 \, T_{cl}$ (7)

$T_{cl} = T_c / (1 - T_{bc} A_s . A_c)$ (8)

$T_c = 1 - A_c - A_c \, m \, \mu_0$ (9)

$A = A_{ray} + T_{2top} A_c + A_s T_2 T_c^2 / (1 - T_{bc} A_s . A_c)$ (10)

with

E	: surface solar irradiance
E_0	: solar constant
T_a	: clear sky atmospheric transmittance (sun-surface with multiple scattering)
T_1	: sun-surface atmospheric transmittance, without multiple scattering
T_2	: sun-surface-satellite transmittance
T_{2top}	: sun-cloud-satellite transmittance
T_{bc}	: transmittance below cloud, a constant value of 0.96 is assumed
A_{ray}	: Rayleigh albedo
A_s	: surface albedo
A_c	: cloud albedo
T_c	: cloud transmittance
T_{cl}	: cloud factor
m	: cloud absorption factor

For a clear pixel, equation (6), the TOA solar irradiance is attenuated by the clear sky atmospheric transmittance. The TOA albedo is not used, the satellite data are used only through the cloud classification.

For a cloudy pixel, the SSI is derived from the TOA albedo through equations (7) to (10). Equation (7) express the SSI as the TOA solar irradiance attenuated by an atmospheric transmittance and a cloud factor, which depends on the cloud transmittance and cloud albedo (equation (8)). Equation (9) relates the cloud transmittance and the cloud albedo, assuming that the cloud absorption linearly depends on the cloud albedo with a constant coefficient m. The TOA albedo, equation (10), is the sum of three terms: Rayleigh scattering, radiation reflected by cloud and attenuated by the atmosphere and radiation reflected by the surface and attenuated by the atmosphere and the cloud. As the TOA albedo is known, solving equations (9) and (10) allows to calculate the cloud albedo and the cloud transmittance. The SSI is then calculated by equations (8) and (7).

2.4.2. Surface albedo

The sea surface albedo is calculated theoretically, while the land surface albedo is derived from an atlas. They vary with respect to the sun zenith angle, after Briegleb et al., 1986 formulas.

land $A_S = A_S(0)\ (1+2d) / (1+2d\ \mu_0)$ $d = 0.4$ (11)

sea with clear sky : $A_S = 0.026/(0.065+ \mu_0^{1.7}) + 15.0\ (\mu_0-0.1)\ (\mu_0-0.5)\ (\mu_0-1.)$ (12)

sea with cloudy sky : $A_S = 0.06$ (13)

2.4.3. Atmospheric transmittances

All atmospheric transmittances are obtained by analytical formulas, depending on viewing angles, atmospheric parameters.

The sun-surface atmospheric transmittance, T_a and T_1, are calculated after Frouin and Chertock, 1992, by the following equations :

$$T_1 = e^{-\tau_{h2o}}\ e^{-\tau_{o3}}\ e^{-\tau_{sc}} \quad (14)$$

$$T_a = T_1 / [\ 1 - A_S\ (\ a' + b'/ V)\ ] \quad (15)$$

$$\tau_{h2o} = 0.102\ (W / \mu_0\ )^{0.29} \quad (16)$$

$$\tau_{o3} = 0.041\ (\ U_{o3} / \mu_0\ )^{0.57} \quad (17)$$

$$\tau_{sc} = (a + b / V) / \mu_0 \quad (18)$$

with

W total water vapor content of the atmosphere in $g.cm^{-2}$

U_{o3} total ozone content of the atmosphere in cm atm

V horizontal visibility in km

a, b, a', b' : coefficients depending on the aerosol type

maritime :	a = 0.059	b = 0.359	a' = 0.089	b' = 0.503
continental :	a = 0.066	b = 0.704	a' = 0.088	b' = 0.456

Equation (18) accounts for multiple scattering between surface and cloud, using a climatological aerosol background.

The double path atmospheric transmittances, T_2 and T_{2top}, differ only by the water vapor absorption, the water vapor content above cloud is assumed to be 30% of the total content. The ozone and water vapor absorption and the Rayleigh scattering formulas are from Lacis and Hansen, 1974 .

$$T_2 = 1 - a_{o3}(U_{o3}\ M)\ - a_{h2o}(W\ M)\ - A_{ray}(\mu_0) - A'_{ray}(\mu) \quad (19)$$

$$T_{2top} = 1 - a_{o3}(U_{o3}\ M) - a_{h2o}(0.3\ W\ M) - A_{ray}(\mu_0) - A'_{ray}(\mu) \quad (20)$$

$$a_{h2o}(x) = 2.9\ x / (1. + 141.5\ x)^{0.635} + 5.925\ x \quad (21)$$

$$a_{o3}(x) = a_{o3}^{VIS}(x) + a_{o3}^{UV}(x) \quad (22a)$$

$$a_{o3}^{VIS}(x) = 0.02118\ x / (1. + 0.042\ x + 0.000323\ x^2) \quad (22b)$$

$$a_{o3}^{UV}(x) = 1.082\ x / (1. + 138.6\ x)^{0.805} + 0.0658\ x\ / [\ 1 + (103.6\ x)^3\ ] \quad (22c)$$

$$A_{ray}(\mu_0) = 0.28 / (1 + 6.43\ \mu_0) \quad (23)$$

$$A'_{ray}(\mu) = 0.0685. \quad (24)$$

where

$$M = (1 / \mu_0 + 1 / \mu)$$

$\mu = \cos(\theta)$ θ being the satellite zenith angle

The formulations of the single path and double path transmittances differ, as a result from a study on a matchup data set gathering GOES-East data and pyranometer measurements (Brisson et al., 1999). On clear sky cases, better SSI results were obtained with Frouin and Chertock, 1992 formulas (equations (14)-(18)). On cloudy cases, the calculated minimum and maximum albedos agree better with observed satellite values, when using Lacis and Hansen, 1974 formulas (equations (19)-(24)).

The cloud absorption factor, m in equation (9), has been tuned on actual satellite data. The tuned value is not fully independent of the radiometer calibration, however the values obtained in several experiments were rather close (Le Borgne et al., 2005). The OSI SAF operational chain has used 0.15 as of March 2005, for GOES-East and MSG imagers. This value will be used for ABI.

2.4.4. Sun glint algorithm

The preliminary step is to identify the pixels affected by sun glint. This step is done with the method used in the NWC cloud classification scheme. In case of sun glint, the clear sky SSI is calculated with equation (6) and a specific scheme is applied to the cloudy pixels.

The bi-directional reflectance $R_{PCocean}$ of the type “partly cloudy over ocean” (Manalo-Smith et al. 1998 formulas) and the cloud type are used to identify the pixels affected by an important sun glint. For these pixels, the cloud albedo A_c is not calculated with equations (9)-(10) but assumed, otherwise the usual algorithm, equations (7)-(10), is used. The cloudy pixels processing can be summarized as follows:

if (fractional cloud or thin cirrus) and ($R_{PCocean} > 0.2$)

$A_c = 0.2$

SSI is calculated with equations (7)- (9)

else

SSI is calculated with equations (7)- (10)

This empirical approach has been verified by the fact that, in the present OSI SAF chain, an hourly SSI field does not show artefacts in the sun glint area, which is obvious in the corresponding visible image.

2.5. Satellite dependent equations or coefficients

The visible channel calibration and, to a lesser extent, the narrow to broadband conversion depend on the satellite radiometer. This section reviews the satellites processed for OSI SAF radiative fluxes The same approach has been used for the Meteosat satellites (MSG with SEVIRI radiometer), but there are a few differences between the GOES-East satellites.

2.5.1. Meteosat satellites

Calibration of SEVIRI visible channel

According to Rogers and Pili, 2001 and to Pili, 2002 (personal communication), the calibration equation, (1), of SEVIRI 0.6 µm visible channel can be written as follows:

$$L_{SC} = (cal\_offset + cal\_slope\ C) / f \qquad (1a)$$

with

C : radiometer count

cal_offset : calibration offset of SEVIRI level 1.5 header, in mW m^{-2} sr^{-1} $(cm^{-1})^{-1}$

cal_slope : calibration slope of SEVIRI level 1.5 header, in mW m^{-2} sr^{-1} $(cm^{-1})^{-1}$

f : radiance to reflectance factor, f= 21.21 mW m^{-2} sr^{-1} $(cm^{-1})^{-1}$ for the 0.6 µm channel (Pili, 2002, personal communication)

The calibration coefficients of SEVIRI level 1.5 data are updated several times per year, as a result of the vicarious calibration method presented in Govaerts and Clerici, 2003. However, the correspondence between the level 1.5 values and those in Govaerts and Clerici, 2003 has not been explicitly presented and is not straightforward (different units, intermediate constants not given and, likely, different offset calculation). The radiometer drift is taken into account in the level 1.5 calibration coefficients.

Narrow to broadband band conversion

The SEVIRI narrow to broadband band coefficients (to be used in equation (4)) are based on the well-calibrated broadband radiometer CERES (Clouds and Earth's Radiant Energy System). They have been obtained by regression on Meteosat-8/SEVIRI and CERES co-located data, supplied by Nicolas Clerbaux. They have been applied to Meteosat-8 data (since 8 March 2005), to Meteosat-9, to Meteosat-10 and to Meteosat-11..

	cloud over ocean	cloud over vegetation	cloud over desert
M	0.819	0.774	0.814
B	0.023	0.063	0.030

***Table 3*:** SEVIRI narrow to broadband band coefficients.

All pixels are considered as cloudy in the narrow to broadband band conversion. This short cut is possible because the visible channel data are ignored for clear pixels (see 2.4).

2.5.2. GOES-East satellites

Calibration of GOES visible channel

In the case of GOES-E, the calibration equation (1) can be written by one of the following equations:

$$Lsc = \alpha\, a\, [\, 1 + b\,(t - t_0)\,]\,(C - C_0) \qquad (1c)$$

or $$Lsc = \alpha\, a \exp[b\,(t - t_0)\,]\,(C - C_0) \qquad (1b)$$

with

- C : radiometer count
- C_0 : radiometer space count
- α : pre-launch calibration coefficient
- a : calibration correction coefficient valid at t_0 ($count^{-1}$)
- b : radiometer drift ($count^{-1} day^{-1}$ or $count^{-1}\ year^{-1}$)
- t_0 : reference time
- t : current time

Equation (1b) is the correct formula, which is used at NOAA. Equation (1c) is an approximation, widely used in the past for GOES and Meteosat series, which could be used for a drift estimation obtained with this formula.

The MF operational scheme, which ingests and pre-processes GOES-East data, apply a calibration method defined by NOAA :

- for GOES-12 and GOES-13, the pre-launch calibration coefficients are used; they are available in Weinreb and Han, 2009 (they slightly differ for the eight detectors of the visible channel)
- for GOES-16, the scaled radiance is obtained through the CSPP Geo software (Community Satellite Processing Package for Geostationary Data http://cimss.ssec.wisc.edu/csppgeo/).

As some defaults have been observed on the GOES visible calibration, the OSI SAF processing chain applies an empirical calibration correction, as presented below.

GOES-12 visible channel has been inter-calibrated against METEOSAT-8 at 37.5W, following the method described in Le Borgne et al. 2004, leading to a corrective factor to be applied to the pre-launch calibration coefficients and to a drift estimation.

GOES-13 became operational on 14 April 2010. As the method used for GOES-12 does not allow a rapid calibration, an empirical approach has been followed. Firstly, a positive bias was observed on the validation stations with GOES-13 on 15-30 April (compared to a negligible bias with GOES-12 on 1-13 April), secondly the routine SSI comparison GOES-East minus METEOSAT shows a positive difference starting on 15 April with GOES-13. This leads to a calibration correction coefficient a = 1.11 (without drift, i.e. b = 0). Then GOES-13 calibration has been updated several times with the NOAA post-launch calibration coefficients (http://www.oso.noaa.gov/goes/goes-calibration/), leading to the following values:

20 May 2010 a= 1.11 b = 0. t_0: 14 April 2010

15 March 2011	a= 1.1127	b = 0.0558 year^{-1}	t_0: 14 April 2010
9 October 2013	a= 1.1256	b = 0.0358 year^{-1}	t_0: 14 April 2010

GOES-16 became operational in December 2017. At first, no calibration correction was applied, then a correction has been obtained [RD.2] and applied on 26 February 2018. On 23 April 2019, NOAA has applied a correction to the ABI Band 2 that reduces the radiance by 6.92% and the OSI SAF corrective factor has been reset to 1, leading to the following values:

14 December 2017	a= 1.0	b=0 year^{-1}	t_0: 1 September 2017
26 February 2018	a= 0.94	b=0 year^{-1}	t_0: 1 September 2017
23 April 2019	a= 1.0	b=0 year^{-1}	t_0: 1 September 2017

Narrow to broadband band conversion

The GOES-12 versus Meteosat-8 comparison at 37.5W has produced GOES-12 calibration coefficient, as a first step, and narrow to broadband coefficients, as a second step. The results over ocean and over Brazil allow to obtain coefficients, “cloud over ocean” and “cloud over vegetation”, respectively. No data are available close to 37.5W to obtain the “cloud over desert” coefficients, which are taken equal the “cloud over vegetation” values. GOES-12 coefficients have been used also for GOES-13.

	cloud over ocean	cloud over vegetation	cloud over desert
M	0.838	0.801	0.801
B	0.014	0.032	0.032

Table 4: GOES-12 and GOES-13 narrow to broadband band coefficients

The 0.6 µm spectral filters of GOES-16/ABI and SEVIRI are rather close (those of GOES12 and GOES-13 were wider), so the SEVIRI narrow to broadband band coefficients (table 3) are also used for GOES-16.

3. DLI algorithm description

The OSI SAF DLI algorithm is a bulk parameterization combining NWP model outputs and satellite derived cloud parameters, which are cloud types derived from the NWC SAF classification [RD.1] for night time pixels and clear to cloudy SSI ratio for daytime pixels. The formulas are presented below.

$$L = (\varepsilon_0 + (1 - \varepsilon_0)\, C)\, \sigma\, T_a^4 \quad (25)$$

$$\varepsilon_0 = 1-(1+ \xi)\, \exp\{-(1.2 + 3.0\, \xi)^{1/2}\} - 0.05\, (p_0-p) / (p_0-710) \quad (26)$$

$$\xi = 46.5\, (e / T_a) \quad (27)$$

if day $C = 1 - E / E_{clear}$ (28)

if night $C = C_i$ (29)

with
- L : downward longwave irradiance at the Earth's surface (W/m^2)
- ε_0 : clear sky emissivity
- C : infrared cloud amount
- T_a: : near surface air temperature (K)
- σ : Stefan-Boltzmann constant $\sigma = 5.6696\ 10^{-8}\ W\ m^{-2}\ K^{-4}$
- e : near surface surface water vapor pressure (hPa)
- p : surface atmospheric pressure (hPa)
- p_0 : normal atmospheric pressure, 1013.25 hPa
- E : surface solar irradiance (W/m^2)
- E_{clear} : clear sky surface solar irradiance (W/m^2)
- C_i : contribution coefficient of this cloud type

The DLI is calculated as the sum of a clear sky and cloudy sky contributions (equation (25)). The clear sky emissivity is derived from the near surface air temperature and water vapor pressure (equations (26) and (27)), according to the formulation proposed by Prata, 1996. The infrared cloud amount, which gives the cloudy sky contribution, is obtained by two different formulations:

- For daytime cases, equation (28), the infrared cloud amount is deduced from the actual to clear sky SSI ratio, as proposed by Crawford and Duchon, 1999.

- For night time cases, equation (29), the infrared cloud amount is the cloud contribution coefficient of the cloud type covering the pixel.

The DLI cloud types correspond to a simplified cloud classification, merging several types of the NWC SAF detailed cloud classification [RD.1]. The values of the cloud contribution coefficients, presented in table 3, have been adjusted on a 1-year data base (July 97 to June 98) gathering DLI measurements, GOES-8 data and observed air temperature and humidity (Brisson et al., 2000). The NWC SAF detailed cloud types have evolved since 1998 but they have always been merged into the same simplified cloud types.

DLI cloud type	C_i	DLI cloud type	C_i
clear	0	fractional cloud	0.15
low cloud	0.82	volcanic ash	0
medium cloud	0.78	sand cloud	0.52
high opaque cloud	0.72	unclassified	0
thin cirrus	0.11	clear re-classified	0
thick cirrus	0.49	medium dubious	0.15

Table 5 **:** cloud types and cloud contribution coefficients (C_i).

4. Radiative flux processing overview

4.1. Products

The delivered products are hourly and daily products on a 0.05 grid [AD.1].There are several types of radiative flux products, all in netCDF4 format:

1) fluxes in satellite space view at infrared channels resolution, not delivered to users:
   - fluxes directly calculated from FDC data — so-called SAT
   - fluxes interpolated at rounded UT hours — so-called 1H
   - daily fluxes — so-called DAY
2) fluxes re-mapped onto a regular grid, delivered to users:
   - fluxes interpolated at rounded UT hours
   - daily fluxes

   Characteristics of the grid:
   Projection: linear scaling in latitude and longitude
   Resolution: 0.05 degree in latitude and longitude
   Coverage: 60S - 60N; 60 W - 60E

4.2. Hourly calculations

A radiative flux product calculated on the original satellite data is not homogeneous in time. The pixel time varies from north to south, depending on the satellite (about 12 minutes for GOES-16 and MSG data and about 24 minutes for GOES-13 data). This temporal variation cannot be neglected for the SSI, which directly depends on the sun zenith angle. The OSI SAF has chosen to calculate products interpolated at rounded UT hours, which are more user friendly and fully consistent between two different satellites.

First, the radiative fluxes are calculated with the algorithms presented in sections 2 and 3, on data every 30 minutes: at nominal times H – 30 minutes and H for Meteosat satellites and H – 20 minutes and H + 10 minutes for GOES-East, H being a UT rounded hour. This time schedule may evolve in the future. The radiative fluxes are stored in workfiles, which contain, in particular, the cloud albedo obtained with the SSI and the cloud contribution obtained with the DLI.

Then, the radiative fluxes are calculated at H, pixel by pixel. All time dependant parameters (viewing angles, surface albedo, atmospheric absorption) are calculated at H. The cloud albedo and the cloud contribution are interpolated between the values available before and after H, which allows to calculate the SSI and the DLI, respectively.

The interpolation scheme can cope with eventual missing images and produces a value in any case, decreasing the quality level (see 4.4):

- if only one value is available, instead of the before-and-after values, this value is used as of,
- eventually, a default value is used: 0.22 for the cloud albedo and 0.29 for the cloud contribution

4.3. Daily calculation

The daily value is the mean irradiance over a UT day. As the 1H products do not have missing values, the daily DLI is simply the mean of all hourly values in the UT day. The SSI daily integration is slightly more complicate, since it accounts for the sunrise and sun set times, calculated independently for every pixel. The integrated energy received during the solar day is divided by 24 hours. The solar day may be fully included in the UT day or corresponds to two uncompleted solar days: day 1 / night / day 2. This configuration is observed with GOES-East data and marginally with MSG data.

4.4. Quality levels

Similarly to the SST products, each pixel DLI or SSI value, is associated to a quality level expressed on a scale showing 6 values: 0: unprocessed, 1: erroneous , 2: bad, 3: acceptable, 4: good, 5: excellent. The quality level values follow the rules presented below.

The 0 value corresponds most of the time to space, the 1 value corresponds to an error in the software logic and should not occur. The other value meanings depend on the products and are described below.

SSI SAT

5: nominal calculation

4: SSI calculation with a minor problem:

sunglint

TOA albedo too low, case considered as clear

TOA albedo too high, maximum cloudiness assumed, SSI=0

DLI SAT

5: DLI value calculated with the daytime method (SSI ratio)

4: DLI value calculated with the nighttime method (NWC classification)

Values 3 and 2 are unused for the SAT products.

SSI or DLI 1H

The 1H flux value is interpolated between SAT values, as explained in 4.3; its quality level is obtained as follows:

5: interpolation between two SAT values both having a quality level of 5

4: interpolation between two SAT values with quality levels (4,5) or (4,4)

3: interpolation with only one SAT value: sunrise, sunset or missing value

2: no SAT value available, using default cloud albedo or contribution

SSI or DLI DAY

The quality level is the rounded mean of the 1H quality levels associated to the fluxes entering into the daily integration; this produces a value from 2 to 5

4.5. Ancillary and auxiliary data

All data needed for the processing of the radiative fluxes are listed in tables 6 and 7. The data are separated in so-called auxiliary data, which are static (atlas and climatology) and ancillary data, which are dynamic (NWP forecast and satellite products).

Parameter	Source	Use
Air temperature and humidity at 2m, surface pressure	ECMWF NWP forecast	clear sky DLI
Air temperature and humidity profiles	ECMWF NWP forecast	calculate total water vapor content for SSI transmittances
Cloud types	NWC SAF cloud classification	SSI calculation DLI cloud contribution

***Table 6**:* ancillary data

Parameter	Source	Use
Land-sea atlas	World Vector Shoreline	identify land and sea pixels (SSI)
Mean altitude	global atlas GTOPO30	calculate total water vapor content for SSI transmittances
Surface type	CERES land cover type atlas	NB to BB conversion (SSI)
Surface albedo	monthly climatology Csiszar and Gutman, 1999	SSI calculation over land
Specific humidity profiles	Ort monthly climatology	calculate total water vapor content for SSI transmittances
Ozone	TOMS monthly climatology	SSI transmittances
Visibility	latitude and month tabulated Stuhlman et al, 1990	SSI transmittances

Table 7: auxiliary data

All ancillary and auxiliary data are first remapped onto the space view grid and then temporally interpolated at the product time.

The integrated water vapour content is derived from the NWP air temperature and humidity profiles and from the altitude atlas. The specific humidity climatology is used only if the NWP atmospheric profiles are missing.

4.6. Remapping

The OSI SAF distributed products are obtained by remapping at the nearest neighbour the 1H and DAY products onto a regular 0.05° grid. The remapping is a final step, which simply re-distributes the radiative fluxes and quality level values without changing them.

5. Continuous control and validation plan

The OSI SAF operational commitment is to process both a Meteosat at 0° and a GOES-East at 75°W. The control and validation plan is based on these two satellites. Meteosat-8 on Indian Ocean is processed and validated on best effort (see examples in [RD.2]).

5.1. Control

The aim of a continuous control is to make available on a near real time basis (immediately after the production of radiative fluxes) relevant information to detect quickly a problem in the functioning of the chain. The control is performed outside the operational environment. It consists in a series of quicklooks, statistics and graphics (partly visible to external users), which are listed below:

- quicklooks of the hourly and daily DLI and SSI products,
- quicklooks of quality levels for a subset of products,
- statistics of (GOES-East – MSG) difference in the overlapping area are daily calculated . The hourly and daily DLI and SSI statistics are plotted as a function of time (figure 1).

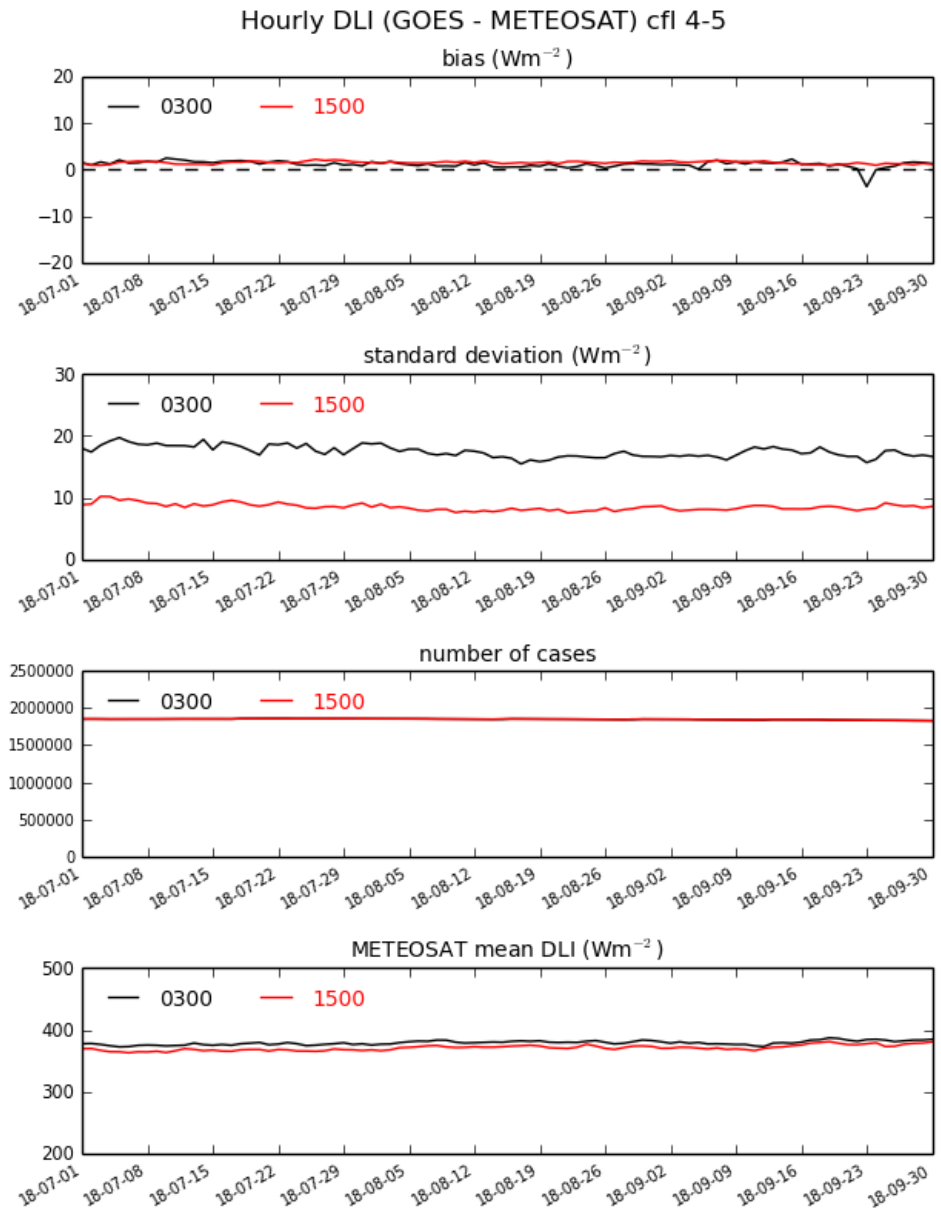

Figure 1: hourly DLI differences, GOES-East minus METEOSAT, at 03:00 UT and 15:00 UT

5.2. Validation plan

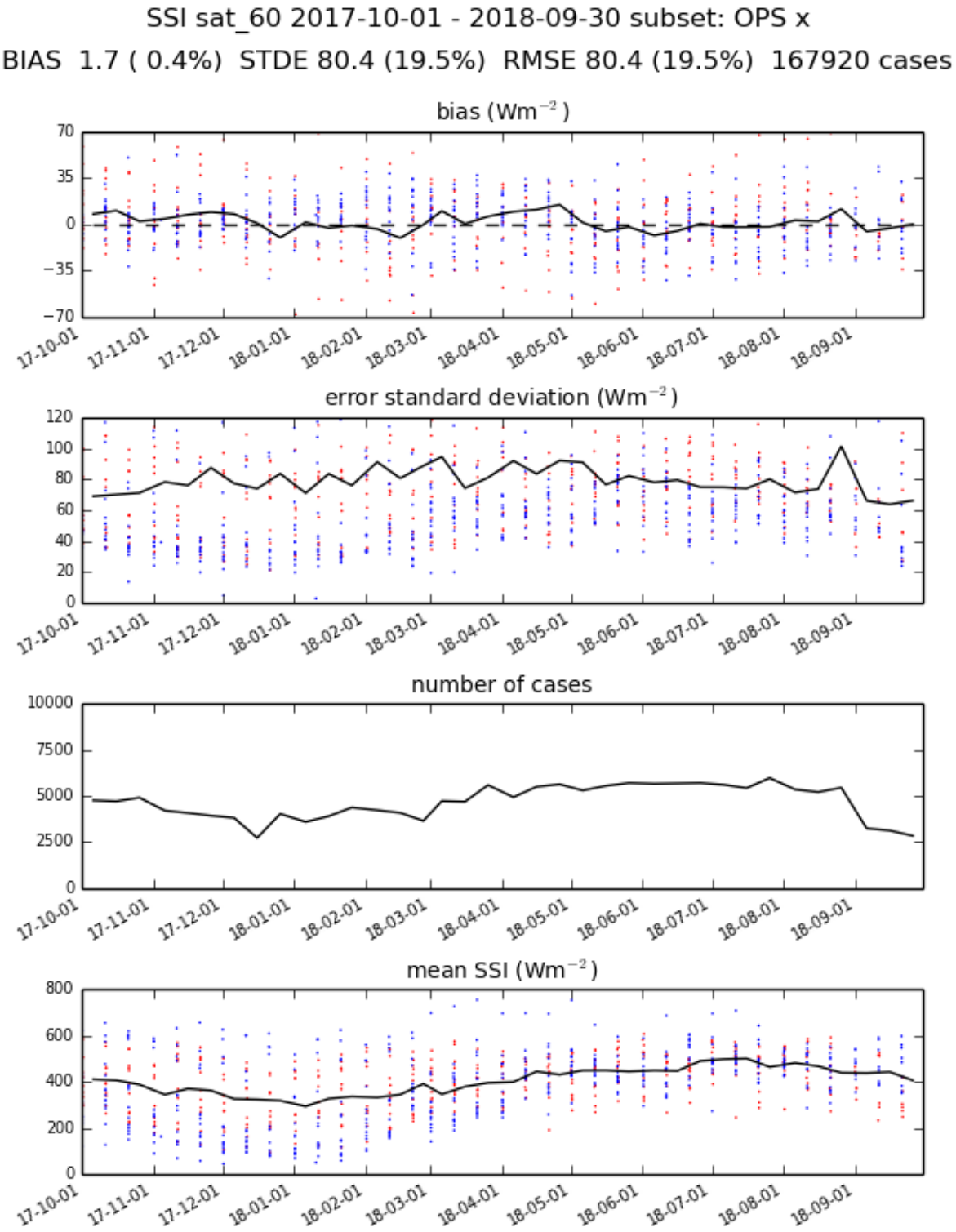

The validation of GOES-East and MSG products is based on Match-up Data Sets (MDS) gathering coincident satellite data and in situ measurements, from pyranometer (SSI) or pyrgeometer (DLI).

The operational validation is done a monthly basis, because some station networks deliver their data at this frequency.

In addition to the operational validation of GOES-East and MSG products, specific validation reports such as [RD.2] are produced, especially in case of a new satellite being processed.

5.2.1. The Matchup data set

MDS files are built routinely for the SAT, 1H and DAY products over a current set of stations, coming from several networks. The satellite data are ingested in near real time and the in situ measurements with a longer delay (one month to several years). Fixed or mobile stations can be added offline into the MDSs, in order to process easily data from oceanographic campaigns.

The measured flux in the MDS is a value centered on the time of the satellite data, obtained from the original in situ data by integration or interpolation. The calculated flux and its quality index are stored on a 9-pixel square box (18 km at sub-satellite pixel) centered on the measurement station. Two options are prepared for the satellite versus in situ comparison in the SAT and 1H MDS:

a. the calculated flux averaged over the box versus the measured flux integrated over 1 hour.

b. the calculated flux at the central pixel of the box versus the measured flux integrated over 10 minutes

Option a has been used for all OSI SAF radiative flux products, option b is more natural from a user point of view (Ineichen et al., 2009).

The SAT MDS files contains complementary data, such as the parameters used in the processing and meteorological measurements at the station.

5.2.2. Statistics

The operational validation is done as follows:

- on a monthly basis, which is the delivering frequency of some measuring networks
- MSG and GOES-East results are merged, due to the limited number of stations,
- two sets of stations (one for SSI and one for DLI) are defined, gathering stations rather well distributed in the area and delivering their measurements in a reasonable delay (figure 2).

Basic statistics of the SSI or DLI difference (calculated minus measured) are computed for all products (SAT, 1H, DAY), per station and for sets of stations.

Graphics , relative to the SSI and DLI operational sets of stations, are produced:

- scatterograms of calculated flux vs measured flux,
- monthly mean and standard deviation of the flux difference, in percentage of the mean measure (figure 3),
- mean and standard deviation of the flux difference as a function of time (figure 4),
- mean and standard deviation of the flux difference per station (figure 5).

Most of the graphics are visible to the users.

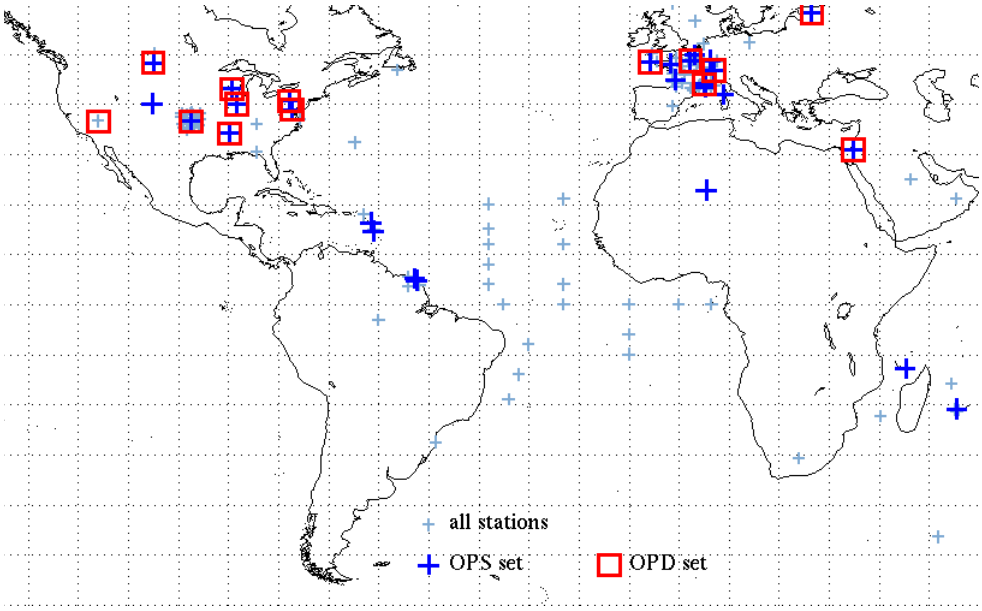

Figure 2: map of the pyranometer and pyrgeometer stations used in 2017-2018, OPS is the operational set for SSI validation, OPD the operational set for DLI validation

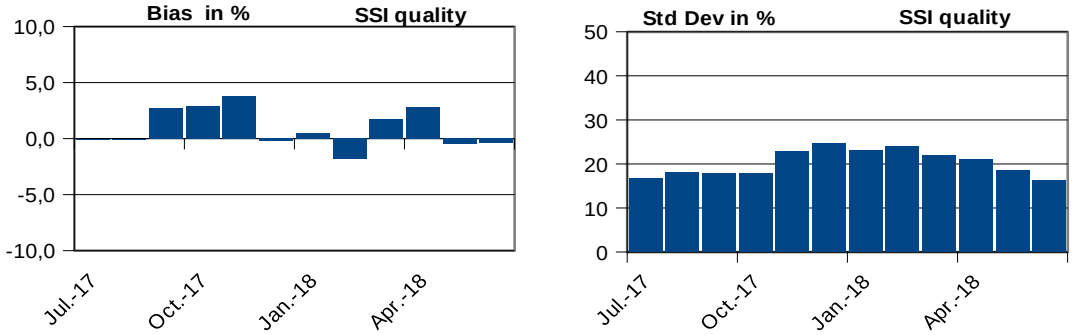

Figure 3: hourly SSI monthly statistics over 1 year, in percentage of the mean measure, from [RD.3]. The left plot shows the mean of the SSI difference and the right plot shows the standard deviation.

Figure 4: hourly SSI validation statistics on a 1-year period

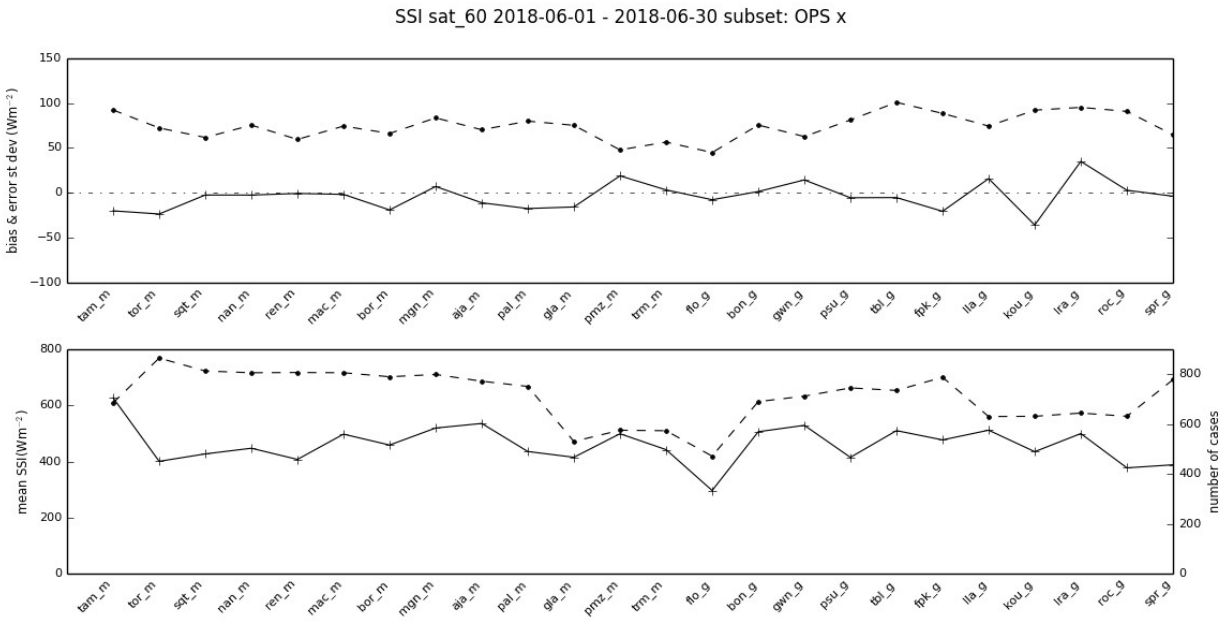

Figure 5: hourly SSI validation statistics per station in June 2018, upper plot showing mean (solid) and standard deviation (dashed) of the SSI difference and lower plot mean SSI (solid) and number of cases (dashed).

6. References

Briegleb B. P., P. Minnis, V. Ramanathan and E. Harrison, 1986, Comparison on regional clear-sky albedos inferred from satellite observations and model computations, Journal of Climate and Applied Meteorology, 25, 214-226.

Brisson, A., P. LeBorgne, A. Marsouin, 1999, Development of algorithms for Surface Solar Irradiance retrieval at OSI SAF low and Mid Latitude, February 1999. Météo-France/DP/Centre de Météorologie Spatiale, BP 147, 22302 Lannion, France.

Brisson, A., P. LeBorgne, A. Marsouin, 2000, Development of algorithms for Downward Long wave Irradiance retrieval at O&SI SAF Low and Mid Latitudes, O&SI SAF Report to EUMETSAT.

Crawford T.M. and C.E. Duchon, 1999, An improved parameterization for estimating effective atmospheric emissivity for use in calculating daytime downwelling longwave radiation. Journal of Applied Meteorology, 38, 474-480.

Csiszar I. and G. Gutman, 1999, Mapping global land surface albedo from NOAA AVHRR, JGR vol. 104, D6, 6215-6228

Darnell W.L. Staylor, W.F., Gupta, S.K., Ritchey, N.A. and Wilbur, A. C., 1992, Seasonal variation of surface radiation budget derived from international satellite cloud climatology project C1 data, Journal of Geophysical Research, 97, 15,741-15,760.

Frouin R. and B. Chertock, 1992, A technique for global monitoring of net solar irradiance at the ocean surface. Part 1: Model, Journal of Applied Meteorology, 31,1056-1066.

Gautier C, Diak G, Masse S. 1980. A simple physical model to estimate incident solar radiation at the surface from GOES satellite data. Journal of Climate and Applied Meteorology. 19: 1005-1012

Geiger B, C. Meurey C, D. Lajas, L. Franchistéguy, D. Carrer D,and JL Roujean ,2008, Near real-time provision of downwelling shortwave radiation estimates derived fromsatellite observations. Meteorological Applications, 15, pp. 411–420.

Govaerts Y.M. and M. Clerici, 2003, Operation Vicarious calibration of the MSG/SEVIRI Solar Channels, EUMETSAT Meteorological Satellite Data Users' conference, Weimar, Germany, 29.09-03.10 2003, pp 147-154.

Gupta, S.K., W.K. Darnell and A.C. Wilber, 1992, A parameterisation for longwave surface radiation from satellite data: recent improvements. Journal of Applied Meteorology, 31,pp. 1361–1367.

Hollmann R, Mueller RW, Gratzki A. 2006. CM-SAF surface radiation budget: First results with AVHRR data. Advances in Space Research. 37: 2166-2172.

Ineichen P. , C.S. Barroso, B. Geiger, R. Hollmann, A. Marsouin and R. Mueller, 2009, Satellite Application Facilities irradiance products: hourly time step comparison and validation over Europe, IJRS, Vol. 30, No. 21, November 2009, 5549-5571

Ineichen P 2010,. *Satellite based short wave irradiance validation over Africa*., Visiting scintist report;

Lacis AA, Hansen JE. 1974. A parameterization for the absorption of solar radiation in the Earth's atmosphere. Journal of the Atmospheric Sciences. 31: 118-133.

Le Borgne P., G.Legendre and A. Marsouin, 2004, METEOSAT And GOES-East Imager Visible Channel Calibration,J. Atmos. Oceanic Technol., 21, 1701-1709.

Manalo-Smith N., G.L. Smith, S. N. Tiwari and W.F. Staylor, 1998, Analytic forms of bidirectional reflectance functions for application to Earth radiation budget studies, Journal of Geophysical Research, Vol. 103, D16, pp. 19,733-19,751, August 27, 1998.

Pinker, R.T., and Laszlo, I., 1992, Modeling surface solar irradiance for satellite applications on global scale, Journal of Applied Meteorology, 31, 194-211.

Prata, A.J., 1996, A new long-wave formula for estimating downward clear-sky radiation at the surface, Quarterly Journal of the Royal Meteorological Society, 122, 1127-1151.

Stuhlmann, R., M. Rieland and E. Raschke, 1990, An improvement of the IGMK Model to derive total and diffuse solar radiation at the surface from satellite data, Journal of Applied Meteorology 29, 586-603.

Tarpley JD. 1979. Estimating Incident Solar Radiation at the Surface from Geostationary Satellite Data. Journal of Applied Meteorology. 18: 1172-1181.